CHAPTER 3

Electrical and Ammonia Gas Sensing Properties of Pristine PQT-12 and PQT-12/CdSe QDs Composite Based Organic Thin Film Transistors*

Contents

*Part of this work has been published as:

1. Chandan Kumar et al., "Electrical and ammonia gas sensing properties of PQT-12/CdSe quantum dots composite based organic thin film transistors," IEEE Sensors Journal, vol. 18, no. 15, pp. 6085-6091, 2018.

CHAPTER 3

Electrical and Ammonia Gas Sensing Properties of Pristine PQT-12 and PQT-12/CdSe QDs Composite Based Organic Thin Film Transistors

3.1 Introduction

We have discussed the 2-terminal PQT-12 thin film based MSM structure in Chapter-2 for detecting hazardous gases such as NH_3 and NO_2. Though the flexible MSM sensor has a good gas response for NO_2 gas but its response to NH_3 is not good enough for low-concentration NH_3 detection. In last few years, the organic thin film transistors (OTFTs) have drawn considerable attention for room temperature NH_3 gas detection with an encouraging response resulted from its inherent internal gain mechanism [9], [42], [68], [72], [127], [129]. The OTFTs are also preferable over the commonly used metal oxide based gas sensors due to their low-temperature operation, low-cost and easy fabrication process [9], [62]. A number of polymers in the polythiophene group such as poly(3-hexylthiophene) (P3HT), poly(3, 3‴-dialkylquaterthiophene) (PQT-12) and poly(2,5-bis(3-hexadecylthiophen-2-yl) thieno[3,2-b] thiophene) (PBTTT) have been widely explored in OTFTs for NH_3 gas sensing applications [9], [42], [68], [70], [72], [127], [129]. Among the aforementioned polymers, the PQT-12 is projected as a promising conducting polymer for OTFT based gas sensing applications due its higher mobility and air stability than the other related polymers as discussed in Chapter-1. However, doped conducting polymer film or the composites of polymer as the active channel material in the OTFTs [103], [126] have been reported with improved electrical and gas response over the conventional pristine

polymer based OTFTs. In view of the above, we have investigated the electrical and ammonia gas sensing properties of two types of OTFTs: one consists of the pristine PQT-12 while the other includes PQT-12/colloidal CdSe QDs composite as the active material in OTFT for ammonia sensing. The CdSe colloidal QDs mixed with the PQT-12 polymer solution is deposited on a SiO_2-grown Si substrate by the spin coating method for the channel material of the OTFT device. The CdSe QDs are treated as foreign particles in the p-type PQT-12 to enhance its charge concentration. The electrical and gas sensing properties of the pristine PQT-12 based OTFT and composite based OTFT have been compared. The outline of the rest of this chapter is as follows:

Section 3.2 presents the experimental details regarding the fabrication of the proposed pristine PQT-12 and composite PQT-12/CdSe QDs based OTFT ammonia sensors. Various results and discussion related to surface and structural morphologies of the two types of polymer films as well as electrical and ammonia gas sensing properties of the OTFTs under study are presented in section 3.3. Finally, section 3.4 summarizes the objectives and concludes the major observations of this chapter.

3.2 Experimental Details

3.2.1 Thin film Deposition and OTFT Fabrication

The high-quality CdSe QDs of average particle size of ~4.84 nm having a standard deviation of 8% are synthesised using the hot-injection method as reported in [164]. Heavily doped p-Si <100> substrates (resistivity 0.01-0.02 ohm-cm) are used for fabricating two type of OTFTs: The first type of OTFT uses simply the pristine PQT-12 film as the channel material while the PQT-12/CdSe QDs composite is used as the channel in the second type OTFTs. The heavily doped p-Si substrates are first properly cleaned by using standard wet cleaning method [165]. A thin SiO_2 film (~300 nm) is

then thermally grown using dry oxidation. The SiO_2 surface is modified by dipping the cleaned substrates in a solution of octadecyltrichlorosilane (OTS) in toluene for 12 hours. The OTS coated Si/SiO_2 substrates are washed ultrasonically in toluene and then dried at 150°C for 1 hour to achieve hydrophobic nature on the oxide surface.

The thickness of PQT-12 film plays an important role with the charge transport phenomenon between source and drain of the OTFTs. The drain current of the OTFT sensor is normally increased with increased PQT-12 film thickness whereas a reverse trend is observed for the response of the sensor [79], [80]. Thus, the thickness for both the pristine PQT-12 and composite PQT-12/CdSe QDs films has been optimized to thinnest thickness possible with composite film (~25 nm) for enhanced gas response with a significant drain current of the OTFT sensors under study [70]. A solution of 2 mg PQT-12 completely dissolved in 1 ml anhydrous chloroform is used for depositing the pristine PQT-12 film by a spin coating method on the OTS treated SiO_2 film for fabricating the pristine OTFT. On the other hand, an optimized loading of CdSe QDs is used for PQT-12/CdSe QDs composite film, so that enhanced hole current is obtained. It is found that 50% loading of CdSe QDs in the composite framework provides maximum hole current and minimum electron current [101]. The obtained PQT-12/CdSe QDs composite is deposited on the OTS treated SiO_2 by spin coating method for fabricating the second type of OTFT device. Both the pristine and composite PQT-12 films dried at 110°C under the flow of nitrogen gas. The samples are then loaded in the thermal evaporator for the formation of source/drain contacts by depositing ~60 nm gold films at the rate of ~1 Å/s on the composite PQT-12 and pristine PQT-12 films. The shadow masking technique is used for obtaining the channel width and length of 1 mm and 30 µm, respectively, of the device. The entire back side of the Si substrate is coated with Al for the back-gate contact of the OTFT as shown in Figure 3.1.

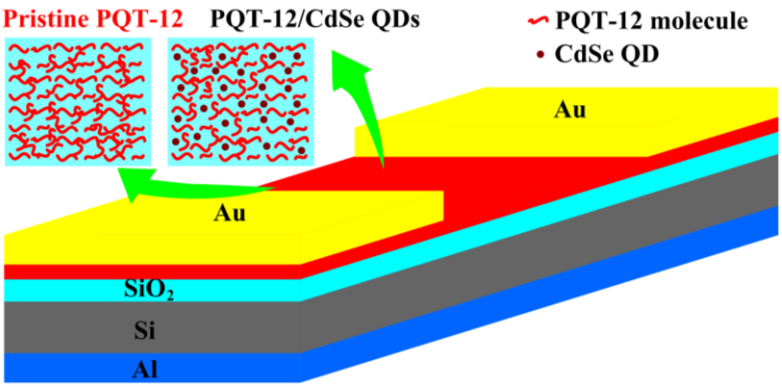

Figure 3.1: OTFT device structure (cross-sectional view) for pristine PQT-12 and PQT-12/CdSe QDs composite film.

3.3 Results and Discussion

In this section, first thin film characterizations and then electrical as well as gas sensing responses of the pristine and composite OTFT sensors are presented and discussed in details.

3.3.1 Thin Film Characterization

The TEM samples for both CdSe QDs and PQT-12/CdSe QDs composite are prepared from their solutions on carbon coated copper grid. The obtained TEM images of CdSe QDs is shown in Figure 3.2 (a). The average particle size of the CdSe QDs is measured from TEM image and found as ~4.84 nm [164]. The SAED pattern with shadow ring shown in the inset of Figure 3.2 (a) confirms the presence of crystalline peak for CdSe. The wrinkles present in the background of TEM image shown in Figure 3.2 (b) confirms the presence of polymer PQT-12 [166]. The hazy ring pattern in the SAED image of the PQT-12/CdSe QDs composite shown in the inset of Figure 3.2 (b) is due to the presence of polymer.

The surface morphology of the optimized ~25 nm thin films of pristine PQT-12 and PQT-12/CdSe QDs composite have been investigated using AFM image shown in Figure 3.3. The surface parameters of the obtained films are compared in terms of peak

to peak spacing, root mean square (RMS) roughness, average roughness, average grain size, and grains length. The obtained surface parameters are listed in Table 3.1 for the comparison. The thin PQT-12/CdSe QDs composite film has more roughness as compared to the pristine PQT-12 film. This increase in surface roughness is due to random distribution of CdSe QDs over the surface. The effective surface to volume ratio of the composite film is larger than that of the pristine PQT-12 thereby implying better gas response of the composite based OTFT than pristine PQT-12 based device [74].

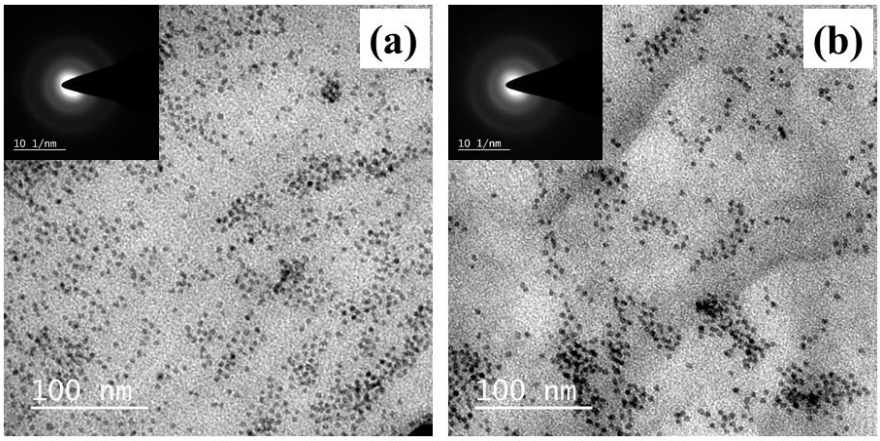

Figure 3.2: TEM topography of (a) CdSe QDs and (b) PQT-12/CdSe QDs composite. The SAED pattern of CdSe QDs in the inset of (a) and PQT-12/CdSe QDs composite in the inset of (b).

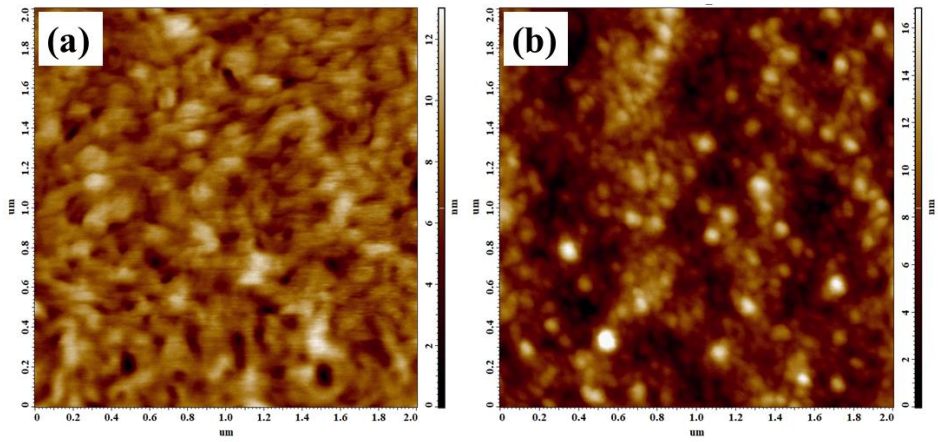

Figure 3.3: AFM topography of (a) pristine PQT-12 film and (b) PQT-12/CdSe QDs composite film.

Table 3.1: Surface parameters for pristine PQT-12 and PQT-12/CdSe QDs composite films.

Parameters/Film	Pristine PQT-12	PQT-12/CdSe QDs composite
Peak to peak spacing (nm)	13.0	16.8
RMS roughness (nm)	1.4	2.5
Average roughness (nm)	1.1	2.0
Average grain size (nm)	44.8	85.3
Grains length (nm)	74.2	131.0

3.3.2 Electrical Characterization

The simplified energy band diagrams have been illustrated in Figure 3.4 for the fabricated transistor structures. The work function of Au (5.1 eV) is aligned with the HOMO level of PQT-12 (5.24 eV) as shown in Figure 3.4 (a). Thus, an ohmic contact is formed for hole injection from Au to PQT-12 at metal/polymer interface, whereas the interface blocks the injection of the electron due to the large band gap of PQT-12 [31], [103], [167]. It is observed that incorporation of CdSe QDs in the PQT-12 film enhance the charge carrier transport due to a decrease in trap density for the holes in the PQT-12/CdSe QDs framework [100], [102], [103]. The mismatch in the HOMO-LUMO levels of PQT-12 and CdSe QDs has also assisted the charge transportation as shown in Figure 3.4 (b). The LUMO level of CdSe QDs is not aligned with the work function of

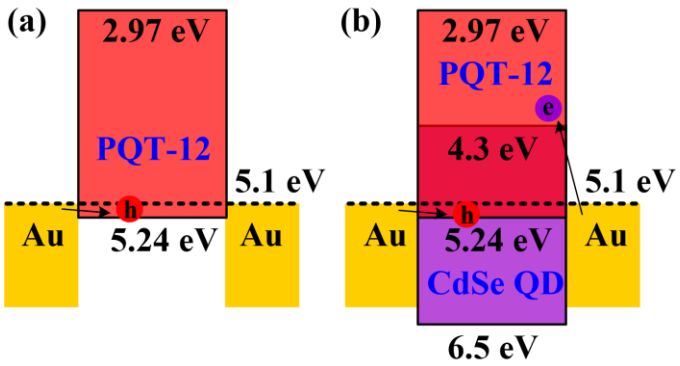

Figure 3.4: Band diagram of (a) Au/PQT-12/Au and (b) Au/PQT-12/CdSe QDs composite/Au under thermal equilibrium.

Au, and this mismatch results in an injection barrier for an electron from Au to CdSe QDs [103], [167]. Thus, the drain current observed in the OTFTs are mainly due to the movements of holes and there is negligible electron current [103].

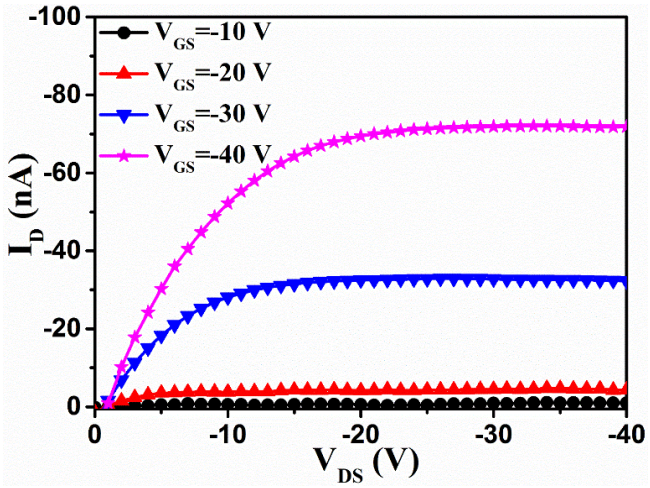

Figure 3.5: Output characteristics of pristine PQT-12 based OTFT.

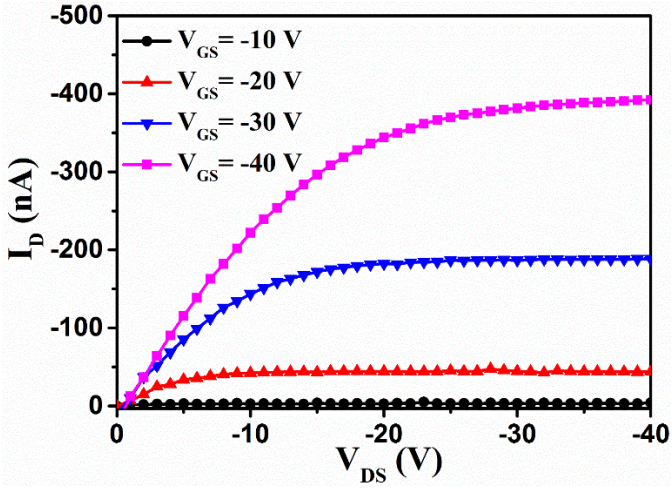

Figure 3.6: Output characteristics of PQT-12/CdSe QDs composite based OTFT.

The output current-voltage characteristics of the fabricated pristine PQT-12 and PQT-12/CdSe QDs composite films based OTFTs measured over the drain voltage range of 0 to -40 V have been shown in Figure 3.5 and Figure 3.6, respectively. The current in the composite film based OTFT is observed much higher than that of the pristine PQT-12 film based OTFT due to the enhanced charge carrier transportation in

the composite film. The built-in field at the PQT-12/CdSe QDs interface also contributes to the enhanced drain current in the composite OTFT device [103]. The drain current at V_{GS} = V_{DS} = -40 V is about four times higher in PQT-12/CdSe QDs composite than the pristine PQT-12 based OTFT. The very low drain currents in both the OTFTs are attributed to the very low thickness of the film and low mobility of the polymer. However, such low currents make the OTFTs suitable for sensing applications [70].

The transfer characteristics of both the OTFTs have been compared in Figure 3.7. The enhanced OTFT performance parameters have been found in PQT-12/CdSe QDs composite OTFT due to enhanced charge carrier transportation. The electrical parameters of the OTFTs such as the field effect mobility (μ), the threshold voltage (V_{th}), on/off current ratio and subthreshold swing (SS) are extracted from the transfer characteristics using the following drain current equation in the saturation region of operation of the OTFT [70], [168]:

$$I_D = \frac{W}{2L}\mu C_i \left(V_{GS} - V_{th}\right)^2 \tag{3.1}$$

which can be written as

$$\sqrt{I_D} = \sqrt{\frac{W}{2L}\mu C_i}\left(V_{GS} - V_{th}\right) = P\left(V_{GS} - Q\right) \tag{3.2}$$

where, I_D is the saturation drain current, L and W are the channel length and width, respectively, C_i is the capacitance per unit area of the SiO_2 layer, and P is the slope of the line $\sqrt{I_D}$ vs. V_{GS}, where $P = \sqrt{\frac{W\mu C_i}{2L}}$ and $Q = V_{th}$

Equation (3.2) gives a linear relation between $\sqrt{I_D}$ and V_{GS} and hence the field

effect mobility can be calculated from the slope the $\sqrt{I_D}$ and V_{GS} plot, while the threshold voltage is obtained by the extrapolation of the line $\sqrt{I_D}$ vs. V_{GS} to *x*-axis where $\sqrt{I_D}$ is zero. The on/off current ratio is computed using $I_{ON} = \left|I_D\left(V_{GS,max}, V_{DS,max}\right)\right|$ and $I_{OFF} = min\left|I_D\left(V_{DS,max}\right)\right|$, while the subthreshold swing is obtained from the slope of the logarithmic plot of I_D vs. V_{GS} as $SS = \max\left|\left(\partial \log_{10}\left|I_D\left(V_{DS,\max}\right)\right| / \partial V_{GS}\right)^{-1}\right|$.

The extracted values of field effect mobility, threshold voltage, on/off current ratio, and subthreshold swing from the transfer characteristic are 1.4×10^{-3} cm^2/Vs, -22.1 V, 3.6×10^{2}, and 7.9 V/dec, respectively, for the pristine PQT-12 film based OTFT, whereas the respective values for the PQT-12/CdSe QDs composite film based OTFT are 4.2×10^{-3} cm^2/Vs, -14.4 V, 1.9×10^{3}, and 5.2 V/dec. The improved performance parameters in a composite film based OTFT are attributed to the built-in field developed due to a mismatch in HOMO-LUMO of PQT-12/CdSe QDs which enhances the charge transport in the composite film [103]. The improvement in charge carrier transport is also observed through the band structure of PQT-12/CdSe QDs shown in Figure 3.4 (b).

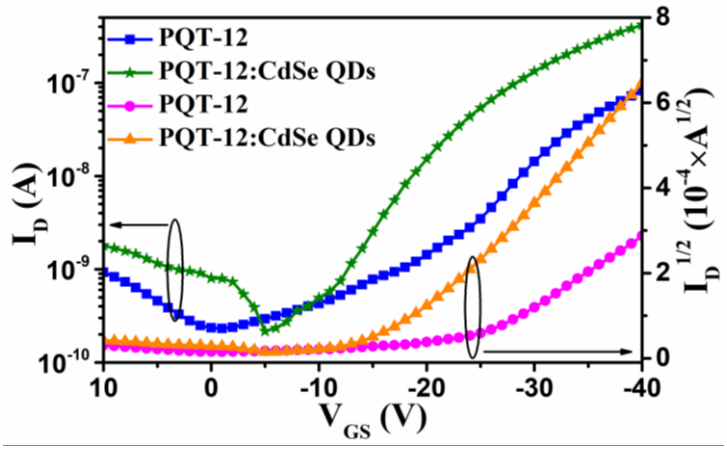

Figure 3.7: Transfer characteristics of pristine PQT-12 and PQT-12/CdSe QDs composite based OTFTs.

3.3.3 Gas Sensing Characterization

The transfer characteristics of the pristine PQT-12 film based OTFTs and PQT-12/CdSe QDs composite film based OTFTs under NH_3 gas exposure are shown in Figure 3.8 and Figure 3.9, respectively. The exposed NH_3 gas is chemisorbed in the PQT-12 polymer film (channel) of the OTFT and disturbs the polymer chain due to the donation of the lone pair from the NH_3 gas [75]. The disturbance in the polymer chain creates the traps in the PQT-12 molecules which, in turn, reduces the hole concentration in the film [68]. As a result, the drain current of the OTFTs is reduced with the increase in NH_3 concentration as observed from Figure 3.8. However, the NH_3 sensing mechanism in the PQT-12/CdSe QDs composite is much complicated since both the materials are responsible for gas response [68], [169] in the device. The measured results in Figure 3.9 show that the PQT-12/CdSe QDs composite film is more sensitive for the chemisorption of NH_3 gas than that of the PQT-12 film due to the larger surface-to-volume ratio as confirmed from the roughness data discussed earlier. While travelling the charge carriers in the channel, they are trapped under NH_3 gas exposure which reduces the charge carrier transport in the channel [128], [170], [171]. The calculated OTFT parameters such as field effect mobility, threshold voltage, on/off current ratio, and subthreshold swing measured under the NH_3 gas exposures of 0 ppm and 100 ppm are listed in Table 3.2.

The gas response (S) of the OTFT sensor is calculated as the ratio of change in drain current ($I_{D,air} - I_{D,gas}$) due to gas exposure to the initial drain current $I_{D,air}$ in ambient air atmosphere [123].

$$S = \frac{I_{D,air} - I_{D,gas}}{I_{D,air}} \times 100\% \tag{3.3}$$

where, $I_{D,gas}$ is the current of the OTFT under NH_3 gas exposure.

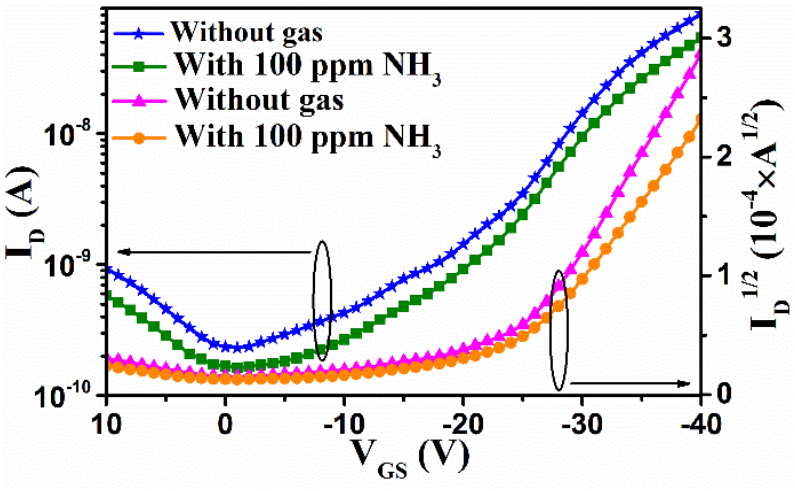

Figure 3.8: Transfer plots of the pristine PQT-12 based OTFT sensor with 100 ppm NH_3 gas.

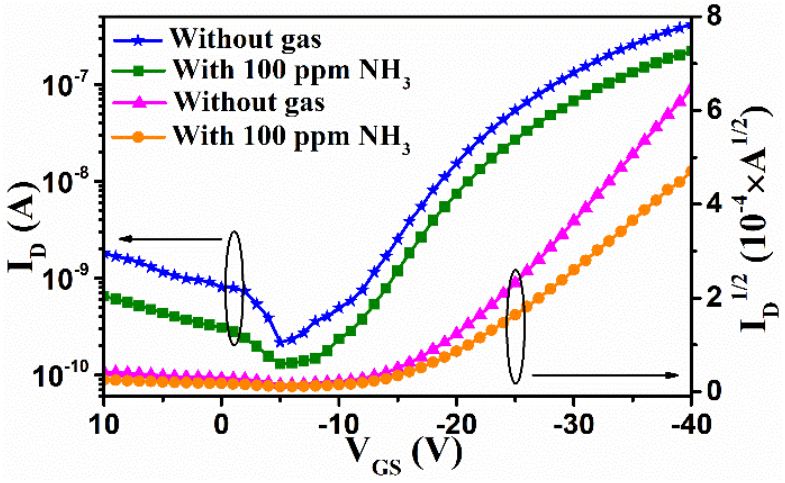

Figure 3.9: Transfer plots of PQT-12/CdSe QDs composite based OTFT sensor with 100 ppm NH_3 gas.

Table 3.2: Electrical parameters of pristine PQT-12 and PQT-12/CdSe QDs composite based OTFT sensors under NH_3 exposure.

OTFTs / **Parameters**	**Pristine PQT-12**		**PQT-12/CdSe QDs composite**	
	Without gas	***With 100 ppm NH_3***	***Without gas***	***With 100 ppm NH_3***
Field effect mobility (cm^2/Vs)	1.4×10^{-3}	1.1×10^{-3}	4.2×10^{-3}	2.8×10^{-3}
Threshold voltage (V)	-22.1	-23.2	-14.4	-16.0
On/off current ratio	3.6×10^{2}	3.3×10^{2}	1.9×10^{3}	1.7×10^{3}
Subthreshold swing (V/dec)	7.9	8.4	5.2	5.9

The gas responses at different concentrations of NH_3 gas from 20 ppm to 100 ppm calculated using Equation (3.3) are plotted as a transient response in Figure 3.10. The maximum gas response of ~41% is obtained for 100 ppm of NH_3 gas in the pristine PQT-12 based OTFT sensor while about ~51% gas response is observed in PQT-12/CdSe QDs composite based OTFT sensor. The PQT-12/CdSe QDs composite based OTFT sensor has a more linear gas response than that of the pristine PQT-12 based OTFT sensor as shown in Figure 3.11. This improved linearity in the gas response is attributed to increased sensor stability due to the incorporation of CdSe QDs in the

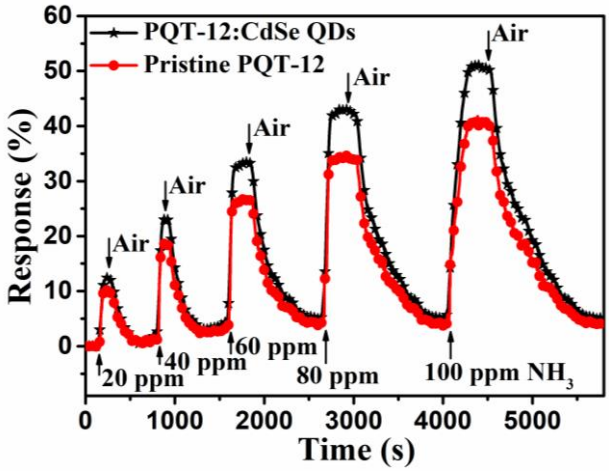

Figure 3.10: Transient response of pristine PQT-12 and PQT-12/CdSe QDs based OTFTs at $V_{DS} = V_{GS} =$ -40 V for different NH_3 gas concentration.

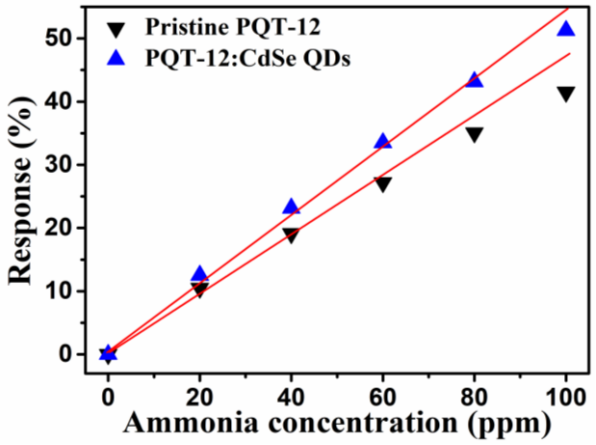

Figure 3.11: Gas responses and fitted line of pristine PQT-12 and PQT-12/CdSe QDs composite based OTFTs at $V_{DS} = V_{GS} =$ -40 V for different NH_3 gas concentration.

PQT-12 framework. However, the response time (~65 s) and recovery time (~240 s) for a composite film based OTFT are slightly higher than the response time (~50 s) and recovery time (~200 s) of the pristine PQT-12 film based OTFT sensor. The selectivity plot of the PQT-12/CdSe QDs composite based sensor is shown in Figure 3.12. The fabricated PQT-12/CdSe QDs film based OTFT sensor has a negligible gas response for organic vapours such as methanol and acetone. The sensor has also an excellent NH_3 gas selectivity over other common environmental interference gases such as hydrogen and carbon monoxide.

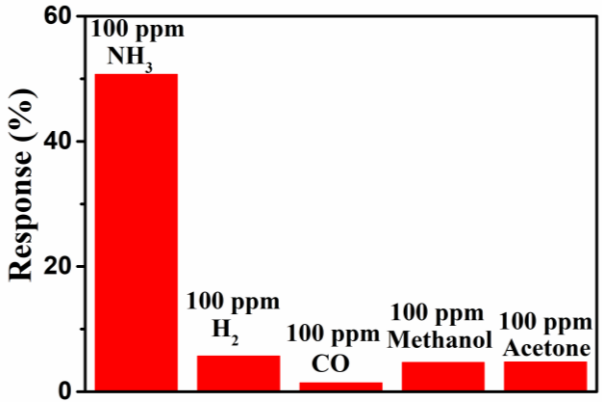

Figure 3.12: Selectivity of PQT-12/CdSe QDs composite based OTFT ammonia gas sensor over common interferences.

3.4 Conclusion

In this chapter, the electrical and ammonia gas sensing properties of the pristine (only) PQT-12 film based OTFT and PQT-12/colloidal CdSe QDs composite film based OTFT have been compared. The OTFT based device provides enhanced ammonia gas response as compared to the MSM sensor considered in Chapter-2. A gas response of ~41% is achieved for 100 ppm of ammonia gas using pristine PQT-12 based OTFT sensor. The use of CdSe QDs/ PQT-12 composite film in the OTFT is observed to have better characteristics over the pristine PQT-12 based OTFT. The field effect mobility, threshold voltage, on/off current ratio, and subthreshold swing are 1.4×10^{-3} cm^2/Vs, -

22.1 V, 3.6×10^{2}, and 7.9 V/dec, respectively, for the pristine PQT-12 film based OTFT, whereas the respective values for the PQT-12/CdSe QDs composite film based OTFT are 4.2×10^{-3} cm^2/Vs, -14.4 V, 1.9×10^{3}, and 5.2 V/dec. The improvements in OTFT parameters are attributed to the enhanced charge transport in the PQT-12/CdSe QDs composite film. The PQT-12/CdSe QDs composite based OTFT has also enhanced ammonia gas response as compared to pristine PQT-12 based OTFT. The PQT-12/CdSe QDs composite based OTFT sensor has the maximum gas response of ~51% at 100 ppm of ammonia gas. It is also observed that the PQT-12/CdSe QDs composite based OTFT sensor has a more linear gas response than that of the pristine PQT-12 based OTFT sensor due to enhanced sensor stability. However, the proposed composite based OTFT has higher response and recovery times than those of the pristine PQT-12 based OTFT ammonia sensor.